Robotica: (2021) volume 39, pp. 1281–1298. © The Author(s), 2021. Published by Cambridge University Press.
doi:10.1017/S0263574720001125

Dual Adaptive Neural Network Controller for Underactuated Systems

Seyed Hassan Zabihifar†*, Hamed Navvabi‡ and Arkady Semenovich Yushchenko†

†*Faculty of Mechatronics and Robotics, Bauman Moscow State technical university (BMSTU), Moscow, Russia. E-mail: navvabi_hamed@mecheng.iust.ac.ir*
‡*Faculty of Mechanic Engineering, Iran University of Science and Technology (IUST), Tehran, Iran. E-mail: yusch@bmstu.ru*

(Accepted November 17, 2020. First published online: February 5, 2021)

SUMMARY
A new stable adaptive controller based on a neural network for underactuated systems is proposed in this paper. The control scheme has been developed for two underactuated systems as examples. The Furuta pendulum and the Inertia Wheel Pendulum (IWP) have been examined in this paper. The presented approach aims to address the control problem of the given system in swing up, stabilization, and disturbance rejection. To avoid oscillations, two adaptive neural networks (ANNs) are implemented. The first one is used to approximate the equivalent control online and the second one to minimize the oscillations.

KEYWORDS: Adaptive neural network; Oscillation compensation; Rotary inverted pendulum; Furuta; Inertia wheel pendulum.

1. Introduction

The nonlinearity of robot dynamics makes the analysis even more complex and difficult than the control of linear dynamic systems. Until now, various approaches are proposed for the control of the uncertain systems, for example, the adaptive control adaptive control,[1–3] variable structure sliding (VSS) control,[4–6] and robust control.[7,8] Robust control methods have been widely studied and employed in many applications such as robotics, vehicles, vibrational systems, electrical systems, aerospace. These methods are effective in handling uncertainty and disturbance to preserve the closed-loop performance. In the presence of uncertainties, we need a robust control method to achieve the desired performance. The goal of robust control is to overcome the imperfection of models including uncertainties and external disturbances.

It has been shown that multi-layer neural networks (NN) can approximate any continuous function as accurately as possible. Based on this universal approximation property, many important adaptive neural network-based control schemes have been developed to solve highly nonlinear control problems including many industrial applications for the tracking control of robot manipulators with uncertainties.[9,10] The adaptive neural network has been applied to achieve control goals due to their approximation property, and the sliding surface brings us robustness property. Regarding the stabilization problem, neural networks have been used in various pendulum-type systems.[11,12] The robustness property of neural networks has been demonstrated using either real-time experiments or numerical simulations. In,[13] adaptive neural network control for unknown nonlinear systems was proposed. The approach was applied to a car pendulum, therein providing tracking of the pendulum without considering the cart's position. In,[14] a dynamic Takagi–Sugeno–Kang-type, radial basis function-based neural fuzzy system was proposed for online estimation of an ideal controller.

* Corresponding author. E-mail: zabihifar@student.bmstu.ru

https://doi.org/10.1017/S0263574720001125 Published online by Cambridge University Press

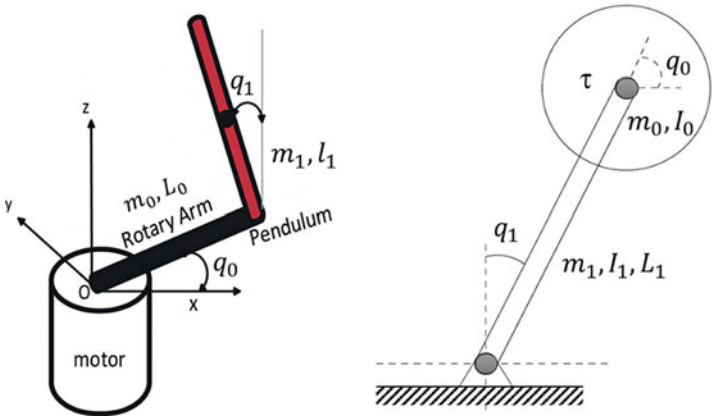


Fig. 1. The Furuta pendulum (left) and IWP (right) systems.

Although the controller can solve a tracking problem, it was applied to the stabilization of the cart-pole system; however, similar to,[13] the boundedness of the cart position was not shown. In,[15] a method based on neural networks with output feedback control was applied to address the tracking problem for a spherical inverted pendulum.

The inertia wheel pendulum is a benchmark for nonlinear control of underactuated mechanical systems.[16] This mechanical system consists of a physical pendulum with a symmetric disk attached to the tip, which is free to spin about an axis parallel to the axis of the rotation of the pendulum. Underactuated nature occurs because it has two DOFs and only one actuator located at the disc. The Furuta pendulum is a two-degree-of-freedom system with only one actuator. This is an inverted pendulum, classified as a nonlinear, non-minimum phase, and underactuated system. The structure is composed of an arm, attached to a motor, rotating in the horizontal plane. At the end of the arm, a pendulum is attached with a free rotational movement in the vertical plane.

Stabilization of a Furuta pendulum has been considered as an active research area to control the engineers' system. The rotary inverted pendulum is a popular testbed for the class of under-actuated mechanical systems. Early researches on rotary inverted pendulum were motivated by the need to design controllers to balance the rockets during a vertical takeoff.[17] Nevertheless, the control algorithm developed for a rotating pendulum system can be easily extended for any other two-degrees-of-freedom unstable underactuated system (e.g., Acrobot, pendubot, inertia wheel pendulum, cart-pole, etc.).[18]

The motion control of such systems becomes difficult because the control of the overall system should be achieved from the actuated joints to the non-actuated joints.[19] Moreover, the presence of extraneous disturbance in the system has made the control design more complicated.

The rotary inverted pendulum (Fig. 1 left), which was first introduced by Furuta et al.,[20] contains well-known underactuated dynamics and many reports can be found about its stabilization. Most of the controls of the rotary inverted pendulum fall into one of the several categories. For example, some have considered the problem of stabilizing the pendulum around the unstable vertical position.[21–25] Some swung the pendulum from its hanging position to its upright vertical position.[26–29] Some tried to create oscillations around its unstable vertical position[30,31] and some tried to track the trajectory of the arm while the pendulum is in the upright vertical position.[19,32] Therefore, three classical control objectives have been discussed in the literature as follows: (1) swing up, (2) stabilization, and (3) trajectory tracking. This study aims to consider the control problem of swing up the pendulum to its upright vertical position and to stabilize the pendulum around that point.

Several robust controllers were proposed for dealing with uncertainties and disturbances in the underactuated systems. Yu et al.[33] proposed a robust controller to stabilize the Furuta pendulum under bounded perturbation. Khanesar et al.[34] used a fuzzy sliding controller to drive a rotary inverted pendulum to the vertical position subject to compensate bounded uncertainties and disturbances. Park et al.[11] presented a swing up and stabilization control with coupled sliding mode control. In,[35] an adaptive RBF network-based NN controller has been proposed, which combines the SMC robust compensator to control problems for a two-link robot manipulator. In,[21] an adaptive controller has been proposed to balance a rotary inverted pendulum with time-varying uncertainties, and finally in,[19]

https://doi.org/10.1017/S0263574720001125 Published online by Cambridge University Press

the tracking control of pendulum-type systems has been discussed using neural networks. In these approaches, oscillations in outputs or control input signals have not been eliminated, and strong fluctuations exist in control input signals when putting the system in an unstable situation in addition to the high energy consumption. Some have steady-state errors or more fluctuations when the external disturbance has been disappeared.

In this paper, the control input has been smoothed in a steady-state mode using a new approach, and the oscillation of the system has been eliminated in which by using filtered tracking error and a new scheme of adaptive neural network algorithm. Removing discontinuity terms in control law and using a dual neural network make a fast adaptation while reasonable control input is needed. The robustness of the system has been demonstrated by applying external disturbance to drive out the system from the equilibrium position. A fuzzy technique has been presented to increase the effectiveness of the controller to stabilize the system in bigger deviations of the pendulum from the 0 angle up to 60°. The results show that the novel dual adaptive neural network controller performs well while the dynamic model of the system is not needed to design the controller. Finally, the results have been compared with previous works to highlight the controller improvement with the newly presented scheme.

The main contributions are as follows:

1. Introducing a new filtered tracking error for stabilizing the pendulum and keep the arm stable with the zero velocity.
2. Proposing a new fuzzy system that helps to increase the generality of the algorithm for various initial conditions.
3. Proposing a new adaptive control scheme with the fuzzy technique for an underactuated system based on dual neural network
4. Introducing new weight adaptation laws for the second neural network based on the e-modification technique and introducing a pseudo-sigmoid activation function in the corrective controller to compensate for the fluctuations.

2. System Dynamics

The dynamic model of the underactuated robotic system in Euler–Lagrange form can be written as

$$M(q)\ddot{q} + C(q, \dot{q})\,\dot{q} + G(q) = U, \tag{1}$$

where $q = [\,q_0 \quad q_1\,]^T \in \mathbb{R}^{2\times 1}$ is a vector of the states, $M(q) \in \mathbb{R}^{2\times 2}$ is the symmetric positive definite mass matrix, $C(q, \dot{q}) \in \mathbb{R}^{2\times 2}$ is the Coriolis and centrifugal force matrix, $G(q) \in\in \mathbb{R}^{2\times 1}$ is the gravity effect, and $U = [\,u \quad 0\,]^T \in \mathbb{R}^{2\times 1}$ is the control input vector. It is assumed that the q_0 is controlled directly and the q_1 is controlled indirectly, which causes the underactuated system.

If $q_d = [\,q_{0_d} \quad q_{1_d}\,]^T \in \mathbb{R}^{2\times 1}$ is a desired trajectory vector that is physical, twice differentiable, bounded, and slowly varying signal then the error is defined as in (2).

$$e_0 = q_{0_d} - q_0,$$
$$e_1 = q_{1_d} - q_1, \tag{2}$$
$$\|q_d(t)\|, \|\dot{q}_d(t)\|, \|\ddot{q}_d(t)\| \le \zeta, \tag{3}$$

where in (3), ζ is a positive constant.

Dynamic model of the system in (1) can be written in the following form:[19]

$$\begin{aligned}
\frac{d}{dt}q_0 &= \dot{q}_0,\\
\frac{d}{dt}\dot{q}_0 &= f_0 + g_0 u,\\
\frac{d}{dt}q_1 &= \dot{q}_1,\\
\frac{d}{dt}\dot{q}_1 &= f_1 + g_1 u.
\end{aligned} \tag{4}$$

https://doi.org/10.1017/S0263574720001125 Published online by Cambridge University Press

The system given by (4) can be written in terms of the tracking error (2) as follows:

$$\dot{e}_0 = \dot{q}_{0_d} - \dot{q}_0, \tag{5}$$

$$\ddot{e}_0 = \ddot{q}_{0_d} - f_0 - g_0 u, \tag{6}$$

$$\dot{e}_1 = \dot{q}_{1_d} - \dot{q}_1, \tag{7}$$

$$\ddot{e}_1 = \ddot{q}_{1_d} - f_1 - g_1 u, \tag{8}$$

which describes the open-loop system with $\dot{q}_{1_d} = 0, \ddot{q}_{1_d} = 0$. Here, it is important to introduce a proper function for error to gain the control goal. Then, we propose an output function $r(t) \in \mathbb{R}$ as a filtered tracking error given by

$$r = \dot{e}_0 + \dot{e}_1 + \lambda e_1, \tag{9}$$

where $\lambda > 0$ is a positive definite design parameter. By computing its time derivative, one can obtain

$$\dot{r} = \ddot{e}_0 + \ddot{e}_1 + \lambda \dot{e}_1 \tag{10}$$

substituting (6) and (8) into (10) and simplifying

$$\dot{r} = \ddot{q}_{0_d} - f_0 - g_0 u - f_1 - g_1 u - \lambda \dot{q}_1 = F - Gu, \tag{11}$$

where

$$\begin{aligned} F &= \ddot{q}_{0_d} - \lambda \dot{q}_1 - f_0 - f_1, \\ G &= g_0 + g_1. \end{aligned} \tag{12}$$

Equation (11) can also be rewritten as

$$\frac{\dot{r}}{G} = \frac{F}{G} - u. \tag{13}$$

It is assumed the function $G(q_1)$ is strictly positive, bounded, and continuous such that

$$\frac{1}{2}\left|\frac{\dot{G}}{G^2}\right| \leq \mu, \tag{14}$$

where μ is a positive constant value.[19]

A two-layer neural network can estimate any nonlinear, continuous, and unknown function.[36] Now, according to the universal approximation property of NN, there is a two-layer NN such that:

$$\frac{F}{G} = \mathrm{f(x)} = W^T \sigma\left(V^T x\right) + \epsilon, \tag{15}$$

which V, W are the NN weights, σ is a sigmoid activation function, x is the input vector of the neural network and the approximation error ϵ bounded on a compact set by

$$\|\epsilon\| < \epsilon_N.$$

Now, let an NN estimate of f(x) be given by

$$\hat{f}(x) = \hat{W}^T \sigma\left(\hat{V}^T x\right), \tag{16}$$

where $\hat{V}$, $\hat{W}$ are the matrix of input and output NN weights, respectively, which should be specified given the tuning algorithm. Note that $\hat{V}$, $\hat{W}$ are estimates of the ideal weight values.

The problem is to define a control law that can estimate the system dynamics and robust enough to compensate for disturbances while reaching the control goal. Handling wide ranges of the initial positions of the pendulum and oscillation compensation is another goal for the control system.

https://doi.org/10.1017/S0263574720001125 Published online by Cambridge University Press

3. Controller Structure

In this section, SHL Networks will perform the approximation of the corresponding command. According to the universal approximation theory, the neural network of the SHL type can estimate any nonlinear, continuous, unknown function.[36] Due to the iterative nature of the neural network's training mechanism and due to the high order of complexity of the dynamic model, the neural network may take a relatively long time to converge, which may lead to unstable dynamics or unsatisfactory performance. Henceforth, a robustifying term F_r, corresponding to a PD controller, which injects damping into the system, is introduced.

$$F_r = K_v r \tag{17}$$

with K_v being a positive constant gain. So a novel adaptive neural network-based controller is proposed by the following expression:

$$U = U^* + U_{cor}, \tag{18}$$

$$U^* = \hat{W}^T \sigma\left(\hat{V}^T x\right) + K_v r, \tag{19}$$

where U^* is the equivalent controller which contains SHL neural network and F_r. The U_{cor} is the ideal corrective control that will be presented in the next section.

The optimal weight matrices $\hat{V}$, $\hat{W}$ are unknown, and it is necessary to estimate them by an adaptation mechanism so that the output feedback control law can be realized. The matrices $\hat{W}$ and $\hat{V}$ are the estimation of W and V, respectively.

Assumption. On any compact subset of $\mathbb{R}^n$, the ideal NN weights are bounded so that $\|W\|_F \leq W_m . \|V\|_F \leq V_m . \; with: \; W_m and \; V_m$ are unknown positive constants, $\|.\|_F$ the Frobenius norm and the weight deviations or weight estimation errors are defined as

$$\tilde{V} = V - \hat{V} \qquad \tilde{W} = W - \hat{W}.$$

Define the hidden layer output error for a given x as

$$\tilde{\sigma} = \sigma - \hat{\sigma} \equiv \sigma\left(V^T x\right) - \sigma\left(\hat{V}^T x\right). \tag{20}$$

The Taylor series expansion of $\sigma(x)$ for a given x may be written as

$$\sigma\left(V^T x\right) = \sigma\left(\hat{V}^T x\right) + \sigma'\left(\hat{V}^T x\right)\tilde{V}^T x + O\left(\tilde{V}^T x\right)^2 \tag{21}$$

with

$$\sigma'(\hat{z}) \equiv \left.\frac{d\sigma\,(z)}{dz}\right|_{z=\hat{z}}. \tag{22}$$

The Jacobian matrix and $O(z)^2$ denotes terms of order two. Denoting $\hat{\sigma}' = \sigma'(\hat{V}^T x)$, we have[37]

$$\tilde{\sigma} = \sigma\left(\hat{V}^T x\right)\tilde{V}^T x + O\left(\tilde{V}^T x\right)^2 = \hat{\sigma}\,\tilde{V}^T x + O\left(\tilde{V}^T x\right)^2. \tag{23}$$

E-modification technique is usually used in robust adaptive control, which is applied for improving the robustness of the controller in the presence of the NN approximation error.[38] Hence, the weight adaptation laws based on e-modification technique has been provided by[37]

$$\dot{\hat{W}} = F_w\left(\hat{\sigma} r^T - k\|r\|\hat{W}\right),$$

$$\dot{\hat{V}} = F_v(x r^T \hat{W}^T \hat{\sigma} - k\|r\|\hat{V}) \tag{24}$$

with $F_w > 0$, $F_v > 0$ are the adaptive gains and k is a positive constant. Then the tracking error *r(t)* approaches to zero with *t,* and the weight estimates $\hat{V}$, $\hat{W}$ are bounded.

https://doi.org/10.1017/S0263574720001125 Published online by Cambridge University Press

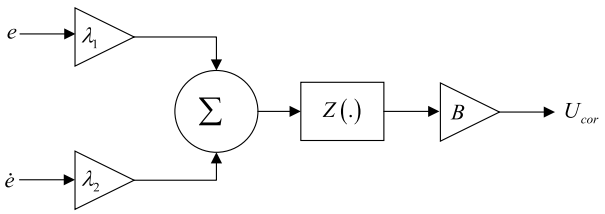


Fig. 2. The second network to estimate the correction term.

3.1. Corrective control

In this section, we have used two techniques to improve the control approach. The first one helps to compensate for oscillations and the second one extends the control ability of the pendulum in bigger deviations from the stable vertical position. Using the sign function to correct the controller makes some oscillations in the steady-state mode that occurs because of discontinuity. Especially when an external disturbance is applied to the system, it will be more dangerous. To eliminate the chattering phenomenon, corrective control is designed. We propose a continuous function *Z(.)* given by

$$Z(x) = \frac{1 - e^{-2x}}{1 + e^{-2x}}. \tag{25}$$

Therefore, the ideal expression of the corrective term will be:

$$U_{cor}^{*} = BZ(\propto^{T} x^{e}), \tag{26}$$

where the gain B and $\alpha = [\,\lambda_1\ \lambda_2\,]^T$ present the ideal output layer and hidden layer weights, respectively, $x^e = [\,e_1\ \dot{e}_1\,]^T$ is the input vector, and Z (.) is the activation function defined in Eq. (25). The second neural network which is shown in Fig. 2 is added to the control scheme. The purpose here is to estimate the ideal corrective term.

The output of this network is represented by

$$U_{cor}^{*} = \hat{B} Z\left(\widehat{\propto}^{T} x^{e}\right) + \varepsilon_c, \tag{27}$$

where $\hat{B}$ and $\widehat{\propto}$ are the estimation of B and $\propto$, respectively, and ε_c is the reconstruction error. The weights B and $\propto$ are unknown, so it is judicious to find a way of adapting them. Therefore, the real estimate of the corrective term by the ANN presented in Fig. 2 has the following structure:

$$U_{cor} = \hat{B} Z\left(\widehat{\propto}^{T} x^{e}\right). \tag{28}$$

The Taylor series expansion of the corrective term for estimation error is given by

$$\tilde{U}_{cor} = BZ - \hat{B}\hat{Z} = \tilde{B}\hat{Z} + B\tilde{Z} = \tilde{B}\hat{Z} + \hat{B}\hat{Z}\tilde{\alpha}^{T} x^{e} + w_g, \tag{29}$$

where $\tilde{B} = B - \hat{B}$, $\tilde{\alpha} = \alpha - \widehat{\alpha}$ are the error parameters. The term W_g presents the approximation error given by

$$w_g = \varepsilon_c + \tilde{B}\hat{Z}'\tilde{\alpha}^{T} x^{e} + \tilde{B} O(\tilde{\alpha}^{T} x^{e})^{2}. \tag{30}$$

Assumption. $\|w_g\| \le \overline{w}_g$, $\overline{w}_g$ is an unknown positive constant and $\|B\| \le B_m$, $\|\alpha\|_F \le \alpha_m$ with α_m and B_m are unknown positive constants. The proposed adaptation laws for adjusting weights are given by the following equations that will be proofed by the Lyapunov function in (40).

$$\begin{aligned} \dot{\hat{B}} &= F_B \hat{Z}\left(\alpha^{T} x^{e}\right) r_e \\ \dot{\widehat{\alpha}} &= F_\alpha \left(x^{e} r_e \hat{B}\hat{Z}' + k_\alpha |r_e| (\overline{\alpha} - \widehat{\alpha})\right), \end{aligned} \tag{31}$$

https://doi.org/10.1017/S0263574720001125 Published online by Cambridge University Press

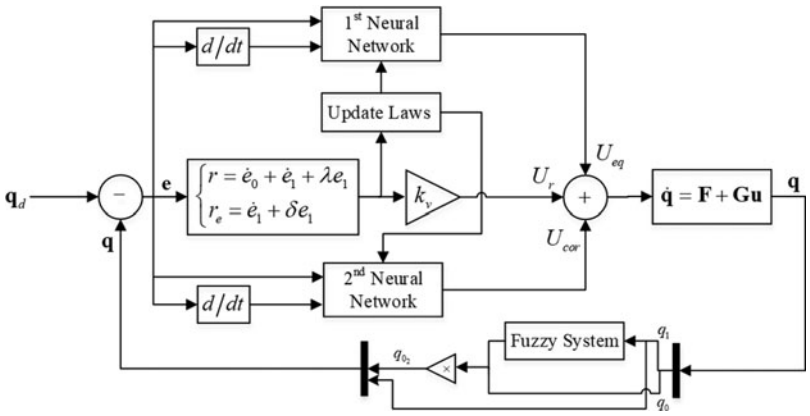


Fig. 3. Control system structure.

where $r_e = \dot{e}_1 + \delta e_1$, $F_B = F_B^T > 0$, $F_\alpha = F_\alpha^T > 0$, $k_\alpha > 0$. The vector $\bar{\alpha}$ is selected as follows:

$$\overline{\alpha} = \left[\frac{p}{|e_1|+\varepsilon} \; 1 \right]^T, \; p, \varepsilon > 0, \tag{32}$$

where $\overline{\alpha} \leq \alpha_n$, α_n is a positive constant. The structure of the controller is shown in Fig. 3.

To increase the generality of the adaptive controller in the various initial angle of the pendulum, a fuzzy technique has been developed. According to the defined filtered tracking error, the derivative of the controllable variable $\dot{e}_0$ has been considered to stable the whole system after reaching the pendulum to the desired position, but it limits the maximum initial deviation of the pendulum from zero. Therefore a fuzzy function has been proposed to eliminate the $\dot{e}_0$ when the e_1 is bigger than 15°.

$$F_{fuz} = 1 - \frac{1}{1 + e^{(15-|x|)}}. \tag{33}$$

Leveraging this technique, the controller able to handle a bigger domain of the initial position of the pendulum. The evaluation results have been shown in the simulation part. It is noticed that this technique has been used only for the Furuta robot because the IWP can be stabilized even when the pendulum is near to the lowest position of about 180°.

3.2. Error system dynamics

The control input from (18), (19), (28) is defined as

$$U = \hat{W}^T \sigma \left(\hat{V}^T x \right) + K_v r + \hat{B} Z \left(\widehat{\alpha}^T x^e \right). \tag{34}$$

Using the control law (34), the closed-loop filtered error dynamics becomes

$$\frac{\dot{r}}{G} = -K_v \, r + \; W^T \sigma \; \left(V^T x \right) - \; \hat{W}^T \sigma \; \left(\hat{V}^T \; x \right) - \hat{B} Z \left(\widehat{\alpha}^T x^e \right) + \varepsilon. \tag{35}$$

Adding and subtracting $W^T \hat{\sigma} \; yields$

$$\frac{\dot{r}}{G} = \; - K_v r + \; \tilde{W}^T \hat{\sigma} + \; W^T \; \tilde{\sigma} - \hat{B} \hat{Z} + \varepsilon \tag{36}$$

moreover, now adding and subtracting $\hat{W}^T \tilde{\sigma}, \; BZ$ yields

$$\frac{\dot{r}}{G} = -K_v r + \tilde{W}^T \hat{\sigma} + \; \hat{W}^T \tilde{\sigma} + \; \tilde{W}^T \tilde{\sigma} + \tilde{B} \hat{Z} + B \tilde{Z} - BZ + \varepsilon. \tag{37}$$

The key step here is the use of the Taylor series approximation for $\tilde{\sigma}$, $\tilde{Z}$ according to which the closed-loop error system is

$$\frac{\dot{r}}{G} = \; -K_v r + \; \tilde{W}^T \hat{\sigma} + \; \hat{W}^T \; \hat{\sigma} \; \tilde{V}^T x + \tilde{B} \hat{Z} + \hat{B} \hat{Z}' \widetilde{\alpha} x^e + w_1, \tag{38}$$

https://doi.org/10.1017/S0263574720001125 Published online by Cambridge University Press

where the disturbance terms are

$$w_1 = \tilde{W}^T \hat{\sigma} \tilde{V}^T x - BZ + w_g + \hat{W}^T O(\tilde{V}^T x)^2 + \varepsilon. \tag{39}$$

As seen, the convergence of "r" to zero implies convergence of the tracking error and its derivative to zero. So, the objective of control is summarized in the synthesis of a control law that allows the convergence of the filtered error to zero.[37] Let the desired trajectory $q_d(t)$ be bounded by q_b. Assume the disturbance term w_1 in (38) equals zero.

Proof. Define the Lyapunov function candidate

$$L = \frac{1}{2}\frac{r^2}{G} + \frac{1}{2} tr\left\{\tilde{W}^T {F_w}^{-1} \tilde{W}\right\} + \frac{1}{2} tr\left\{\tilde{V}^T {F_v}^{-1} \tilde{V}\right\} + \frac{1}{2} tr\left\{\tilde{B}^T F_B^{-1} \tilde{B}\right\} + \frac{1}{2} tr\left\{\tilde{\propto}^T F_{\propto}^{-1} \tilde{\propto}\right\}. \tag{40}$$

Differentiating yields

$$\dot{L} = r\frac{\dot{r}}{G} - \frac{1}{2}\frac{\dot{G}}{G^2} r^2 + tr\left\{\tilde{W}^T {F_w}^{-1} \dot{\tilde{W}}\right\} + tr\left\{\tilde{V}^T {F_v}^{-1} \dot{\tilde{V}}\right\} + tr\left\{\tilde{B}^T F_B^{-1} \dot{\tilde{B}}\right\} + tr\left\{\tilde{\propto}^T F_{\propto}^{-1} \dot{\tilde{\propto}}\right\}. \tag{41}$$

Whence substitution from (38) (with $w_1 = 0$) yields

$$\begin{aligned} \dot{L} = &-K_v r^2 - \frac{1}{2}\frac{\dot{G}}{G^2} r^2 + tr\left\{\tilde{W}^T \left({F_w}^{-1} \dot{\tilde{W}} + \hat{\sigma} r^T\right)\right\} + tr\left\{\tilde{V}^T \left({F_v}^{-1} \dot{\tilde{V}} + x r^T \hat{W}^T \hat{\sigma}\right)\right\} \\ &+ tr\left\{\tilde{B}^T \left(F_B^{-1} \dot{\tilde{B}} - r^T \hat{Z}\right)\right\} + tr\left\{\tilde{\propto}^T \left(F_{\propto}^{-1} \dot{\tilde{\propto}} + x^e r^T \hat{B} \hat{Z}\right)\right\}. \end{aligned} \tag{42}$$

Since $\hat{W} = W - \tilde{W}$, the W is constant, so $d\frac{\tilde{W}}{dt} = -d\hat{W}/dt$ (as for V, B, and $\propto$) the tuning rules from (31), (24) yield

$$\begin{aligned} \dot{L} = &-K_v r^2 - \frac{1}{2}\frac{\dot{G}}{G^2} r^2 + tr\left\{\tilde{W}^T \left(k \|r\| \hat{W}\right)\right\} + tr\left\{\tilde{V}^T \left(k \|r\| \hat{V}\right)\right\} + tr\left\{\tilde{B}^T \hat{Z}(r - r_e)\right\} \\ &+ tr\left\{\tilde{\propto}^T \left(x^e \hat{B} \hat{Z} (r - r_e) - k_\alpha |r_e| (\overline{\alpha} - \widehat{\alpha})\right)\right\}, \end{aligned} \tag{43}$$

$$\begin{aligned} \dot{L} = &-K_v r^2 - \frac{1}{2}\frac{\dot{G}}{G^2} r^2 + k \|r\| tr\left\{\tilde{W}^T \left(W - \tilde{W}\right)\right\} + k \|r\| tr\left\{\tilde{V}^T \left(V - \tilde{V}\right)\right\} \\ &+ tr\left\{\tilde{B}^T \hat{Z}(r - r_e)\right\} + tr\left\{\tilde{\propto}^T \left(x^e \hat{B} \hat{Z} (r - r_e) - k_\alpha |r_e| (\overline{\alpha} - \widehat{\alpha})\right)\right\}. \end{aligned} \tag{44}$$

Define the matrix of all the NN weights as

$$T \equiv \begin{bmatrix} W & 0 \\ 0 & V \end{bmatrix} \tag{45}$$

Assumption. On any compact subset of $\mathbb{R}^n$, the ideal NN weights are bounded so that

$$\|T\|_F \leq T_B$$

with T_B known and $\|\cdot\|_F$ the Frobenius norm. Then

$$\begin{aligned} \dot{L} = &-K_v r^2 - \frac{1}{2}\frac{\dot{G}}{G^2} r^2 + k \|r\| tr\left\{\tilde{T}^T \left(T - \tilde{T}\right)\right\} + (r - r_e) tr\left\{\tilde{B}^T \hat{Z} + \tilde{\propto}^T x^e \hat{B} \hat{Z}\right\} \\ &- k_\alpha |r_e| tr\{(\overline{\alpha} - \widehat{\alpha})\}. \end{aligned} \tag{46}$$

https://doi.org/10.1017/S0263574720001125 Published online by Cambridge University Press

Since $tr\left\{\tilde{T}^T\left(T-\tilde{T}\right)\right\} \leq \|\tilde{T}\|_F\|T\|_F - \|\tilde{T}\|^2{}_F$ there results the following:[37]

$$\begin{aligned}
\dot{L} \leq & -\|r\| K_v \|r\| - \frac{1}{2}\frac{\dot{G}}{G^2}r^2 + k\|r\|.\|\tilde{T}\|_F\left(T_B - \|\tilde{T}\|_F\right) + (r-r_e)\, tr\left\{\tilde{B}^T\hat{Z} + \tilde{\propto}^T x^e \hat{B}\hat{Z}'\right\} \\
& - k_\alpha |r_e|\, tr\{(\overline{\alpha} - \widehat{\alpha})\}, \\
\dot{L} \leq & -\|r\| K_v \|r\| - \frac{1}{2}\frac{\dot{G}}{G^2}r^2 - k\|r\|.\left(\|\tilde{T}\|_F - D\right)^2 + k\|r\| D^2 + (r-r_e)\, tr\left\{\tilde{B}^T\hat{Z} + \tilde{\propto}^T x^e \hat{B}\hat{Z}'\right\} \\
& - k_\alpha |r_e|\, tr\{(\overline{\alpha} - \widehat{\alpha})\}, \\
\dot{L} \leq & -\frac{1}{2}\frac{\dot{G}}{G^2}r^2 - k\|r\|.\left(\|\tilde{Z}\|_F - D\right)^2 - \|r\|\left(K_v\|r\| - kD^2\right) - \left(\overline{w}_g + k_\propto\frac{\propto_m^2}{4} + k_\propto\|\tilde{\propto}\|\,\|\overline{\propto}\|\right)|r_e|, \\
\dot{L} \leq & -\frac{1}{2}\frac{\dot{G}}{G^2}r^2 - k\|r\|.\left(\|\tilde{Z}\|_F - D\right)^2 - \|r\|\left(K_v\|r\| - kD^2\right) - \left(\overline{w}_g + k_\propto\frac{\propto_m^2}{4}\right)|r_e| - k_\propto|r_e|\propto_n^2,
\end{aligned} \tag{47}$$

where $D = \frac{T_B}{2}$. Suppose that $k > 0$, using the inequality in (14) the first term is negative, then we prove that the Lyapunov first-time derivative becomes negative if:

$$\|r\| > \frac{kD^2}{K_v}m$$

Then we prove that the Lyapunov first-time derivative will be:

$$\dot{L} \leq 0,$$

which guarantees the stability of closed-loop system.[19,36,37]

4. Simulation Studies and Performance Comparison

The simulation results are introduced to make it possible to see the operation of the proposed dual adaptive neuro controller and its performance in disturbance rejection. Two underactuated systems that are described, have been evaluated and the results of the swing up the pendulum and disturbance rejection tests are introduced. For robot Furuta, a simulation comparison wherein two controllers are compared with the new controller is performed. For IWP, the proposed approach has been compared with another free model approach, which is called the Adaptive Fuzzy Sliding mode controller (AFSMC) which is developed in.[39] The model parameters are briefly described, and the controllers used in the comparison are introduced. The dynamic model of the Furuta pendulum in Euler–Lagrange form[40,41] can be written as (1), where

$$M(q) = \begin{bmatrix} I_0 + m_1\left(L_0^2 + l_1^2\sin^2 q_1\right) & m_1 l_1 L_0 \cos q_1 \\ m_1 l_1 L_0 \cos q_1 & J_1 + m_1 l_1^2 \end{bmatrix},$$

$$C(q,\dot{q}) = \begin{bmatrix} \frac{1}{2}m_1 l_1^2 \sin(1q_1)\dot{q}_1 & -m_1 l_1 L_0 \sin q_1\, \dot{q}_1 + \frac{1}{2}m_1 l_1^2 \sin(2q_1)\dot{q}_0 \\ -\frac{1}{2}m_1 l_1^2 \sin(2q_1)\dot{q}_0 & 0 \end{bmatrix},$$

$$G(q) = \begin{bmatrix} 0 \\ -m_1 g l_1 \sin q_1 \end{bmatrix}, \quad U = \begin{bmatrix} u \\ 0 \end{bmatrix}$$

and the dynamic model of the Inertia Wheel pendulum (IWP) in Euler–Lagrange form[42] can be written as (1), where

$$M(q) = \begin{bmatrix} I_0 & I_0 \\ m_1 l_{c1}^2 + m_0 l_1^2 + I_1 + I_0 & I_0 \end{bmatrix}, \quad C(q,\dot{q}) = 0,$$

https://doi.org/10.1017/S0263574720001125 Published online by Cambridge University Press

Table I. The model parameters.

The Furuta Pendulum	**The Inertia Wheel Pendulum**
I_0: Inertia of the arm	I_1: Moment of inertia of the pendulum
L_0: Total length of the arm	I_0: Moment of inertia of the disc
m_1: Mass of the pendulum	m_1: Mass of the pendulum
l_1: Distance to the center of mass of the pendulum	m_0: Mass of the disc
J_1: Inertia of the pendulum around its center of mass	l_{c1}: Distance at the center of mass of the pendulum
q_0: Rotational angle of the arm	l_1: Length of the pendulum
q_1: Rotational angle of the pendulum	q_0: Joint position of the disc
u: Input torque applied on the arm	q_1: Joint position of the pendulum
g: The gravity	u: Input torque applied on the disc

$$G(q) = \begin{bmatrix} -(m_1 g l_{c1} + m_0 g l_1) \sin q_1 \\ 0 \end{bmatrix}, \quad U = \begin{bmatrix} u \\ 0 \end{bmatrix}.$$

The coordinate system and notations are described in Fig. 1 and Table I:

4.1. Controllers used in the comparison

A simulation study to assess the performance of the new controller (34) has been performed. Specifically, a linear controller and the adaptive neural network schemes in[43] and[32] were implemented in real time. The schemes in[19,32,43] have an adaptive neural network component and a linear PD or PID component. In addition, in,[19] there is a nonlinear term that eliminates the adaptation error introduced by the neural network but that discontinues term introduces some fluctuations specifically when the disturbance happens. In the proposed controller, the second adaptive neural network has been used to eliminate the oscillation and the adaptation error. Also in disturbance investigation, the external disturbance should be applied on the pendulum to observe the ability of the controller to keep it stable while in some of the previous works, it has been applied as a torque summation in the control input of the first link. In,[19] the initial angle of the pendulum has been defined as zero, while here we propose different nonzero initial angles to highlight the ability of the proposed scheme to swing up ,and also the robustness against external disturbances has been confirmed. It is important to observe that the proposed adaptation laws (24), (31) of the new scheme (34) are derived such that the time derivative of the Lyapunov function L in (40) is negative, and some of the other schemes use the backpropagation adaptation without any motivation given by the closed-loop system analysis.

The adaptive neural network controller proposed by J. Moreno[19] is given by

$$\tau = -\hat{W}^T \sigma(\hat{V}^T x) - k_p y - \delta \, sign(y), \tag{48}$$

where the constants k_p and δ are positive, $\hat{V}$ is the matrix of estimated input weights, and $\hat{W}$ is a vector of the estimated output weights. Output function $y(t)$ is given by

$$y = \dot{e}_1 + \Delta_1 e_1 + \dot{e}_2 + \Delta_2 e_2, \tag{49}$$

where $\Delta = 3$, $\Delta_2 = 8$ are positive constants and $k_p = 1.05$, $\delta = 0.035$. The number of neurons in the hidden layer was L = 10. The adaptation laws were implemented with $\alpha = 1$, N = 1.05, and R = 8.53. The weights of the neural network were initialized to zero. It is worth mentioning that the presented approach by Moreno has been compared with the PID algorithm, and the results show the superiority of Moreno's approach to the PID algorithm. So the PID has not been discussed in this paper.

In the tests, we also consider the adaptive neural network controller proposed by Chaoui and Sicard.[32]

$$\tau = \tau_{NN} + k_D S \tag{50}$$

where τ_{NN} is the output of a two-layer neural network, six neurons in the hidden layer, and one neuron for the output layer, whose input and output weights are obtained by the backpropagation algorithm, which minimizes the signal s given by

$$s = [1 - \lambda]\,[\dot{e}_1 + \psi_1 e_1] + \lambda\,[\dot{e}_2 + \psi_2 e_2] \tag{51}$$

https://doi.org/10.1017/S0263574720001125 Published online by Cambridge University Press

Table II. Dynamic system parameters.

Furuta		**IWP**	
$m_0 = 990\ gr$	$l_0 = 55\ cm$	$m_0 = 300\ gr$	$D_0 = 3.8\ cm$
$m_1 = 225\ gr$	$l_1 = 25\ cm$	$m_1 = 60\ gr$	$l_1 = 14.5\ cm$

Table III. Controller parameters.

Furuta			**IWP**		
$F_w = 100$	$F_B = 5$	$B, W, V = 0$	$F_w = 20$	$F_B = 5$	$B, W, V = 0$
F_v=50	$F_\alpha = 2$	$\lambda_1 = 0$	$F_v = 50$	$F_\alpha = 2$	$\lambda_1 = 0$
k=1	$k_\alpha = 1$	$\lambda_2 = 0$	*k=1*	$k_\alpha = 1$	$\lambda_2 = 0$

with $0 < \lambda < 1, \psi_1, \psi_2 > 0$, and $k_D > 0$. Specifically, (50) was implemented with $\lambda = 0.5$, $\psi_1 = 20$, $\psi_2 = 30$, and $k_D = 1.757$. The details regarding the controllers (48) and (50) can be found in[19] and,[32] respectively. The adaptive fuzzy sliding mode controller is extended for underactuated systems and proposed in.[39]

$$u = \hat{u}^{fuz} + u^{rb},$$
$$u^{rb} = diag\left(\hat{k}\right) sgn(S)\,, \tag{52}$$
$$S = k_1 \dot{e}_1 \cos(e_1) + k_2 \sin(e_1)\,,$$
$$\dot{\hat{k}} = \alpha\,|S|\,, \tag{53}$$

where $\hat{u}^{fuz}$ is the output of fuzzy system to approximate the ideal controller and u^{rb} is employed to compensate the difference between the fuzzy controller and the ideal one. $k_1 = 0.02$, $k_2 = 0.6$, $\alpha = 3$ are preselected positive values.

4.2. Simulation

The simulations have been conducted on a MATLAB® Simulink and the dynamic models have been modeled by the SimMechanics toolbox and all the dynamic parameters and the gravity have been considered as well. The initial conditions and the actual values of the system parameters for both the examples are defined in Table II.

For the proposed controller, the number of neurons in the hidden layer is 7, and the initial values for W and V are assumed to be 0. Determining the number of hidden layer neurons required for the best approximation is an open problem for general fully connected two-layer NN.[37] To achieve an appropriate response, the number of 3–11 hidden layers are defined by the trial-and-error approach.

The adaptive coefficients of (24) and (31) and the initial values of weights for both control systems are defined in Table III.

To stabilize the system, the arm velocity in robot Furuta and the rotation velocity of the wheel in IWP should also be controlled, so by defining the zero as a desired speed of the arm and the wheel, a stable system has been achieved, although for IWP, the priority of the control approach is stabilizing the pendulum and the wheel velocity could be sacrificed for stabilizing the pendulum. Therefore, the state variables are considered as follows:

$$X = \left[e_1 \;\; \dot{e}_1 \;\; e_{1delay} \;\; \dot{e}_0 \;\; \ddot{e}_0\right],$$
$$e_0 = q_{0desired} - q_0,$$
$$e_1 = q_{1desired} - q_1. \tag{54}$$

In this paper, a simple delayed signal, e_{1delay}, is considered in order to consider the dependency of the controller output on past inputs beside the current inputs. In principle, multiple delayed signals can

https://doi.org/10.1017/S0263574720001125 Published online by Cambridge University Press

Table IV. Quantification of results.

	Sicard	**Moreno**	**New**
Max $\{\|e_1(t)\|\}$ [deg.] , 5<t<10	9.9816	7.9396 e-7	7.9127 e-8
Max $\{\|e_1(t)\|\}$ [deg.] , 2<t<10	24.9321	0.0316	0.0144
RMS $\{e_1(t)\}$ [deg.]	14.4649	5.5332	4.1394
RMS $\{U(t)\}$[Nm]	4.0401	142.2150	3.9859
Settling time $q_1(t)$ (2%) [s]	14.28	1.125	1.024

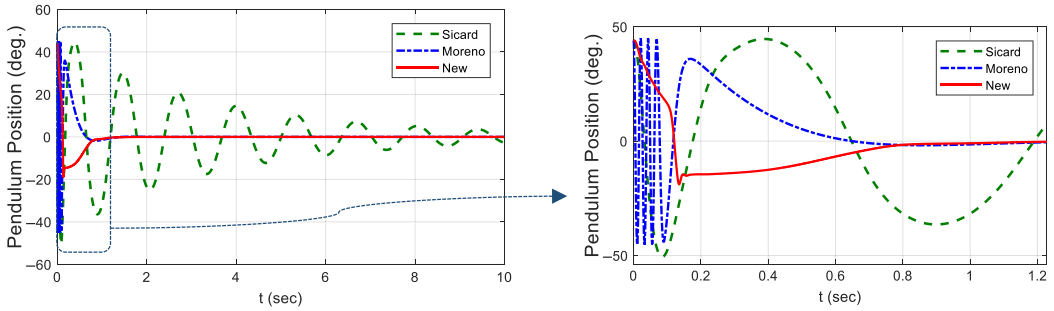


Fig. 4. The angle of pendulum position in comparison with other implemented controllers and the magnified part of it.

be used, but here only one simple delayed signal is introduced. According to Eq. (24), its parameters are calculated as follows:

$$\sigma(x) = \frac{1}{1+e^{-x}}. \tag{55}$$

Then, $\sigma'(x)$ is calculated as follows:[37,44,45]

$$\sigma(x) = \sigma(x)\sigma(-x). \tag{56}$$

4.3. Simulation results for the robot Furuta

In this section, the results are presented. For simplicity, the proposed controller in (34) is labeled as "new", the neural network controller proposed by[19] in (48) is labeled as "Moreno" and the neural network controller introduced by[32] in (50) is labeled as "Sicard.". The results of the three implemented controllers to reach the inverted pendulum from 44° (as the biggest initial position of the pendulum in which all the approaches work) to the vertical position without external disturbances have been shown in Figs. 4 and 5. The maximum absolute value of the pendulum position error and Root Mean Square RMS) value of the error and the control input have been compared in Table IV. The settling time has been defined when the signal crosses into and remains in the 2% tolerance region around the state level. In maximum error quantification, the first time interval is considered after 5s when the pendulum is in a stable position, and the maximum of the error has been highlighted. The second time interval (2<t<10) shows the ability of the proposed approach to reach a stable position in a shorter time.

Figure 4 shows that, in a very short time, the controller can adapt to parameters with a completely unknown model for the controller, and control the underactuated system well. The velocity of the arm is going to zero while there is no oscillation (Fig. 5). The first second of the diagrams have been magnified to highlight the performance of the proposed controller in comparison with others. The fast adaptation, less oscillation in pendulum position, and arm velocity are the advantages of the new controller. Table IV presents a quantification of the results obtained during the tests, therein showing a comparison of the maximum absolute value of the error $e_1(t)$, the RMS value of the error $e_1(t)$, control input $U(t)$, and the settling time for each algorithm. Better performance is obtained with the new controller because the index RMS{e(t), $U(t)$}, the settling time, and the maximum absolute of the error are the lowest.

https://doi.org/10.1017/S0263574720001125 Published online by Cambridge University Press

Table V. Quantification of error with external disturbance.

	Sicard	**Moreno**	**New**
RMS error (deg.)	21.2531	8.4024	6.1720

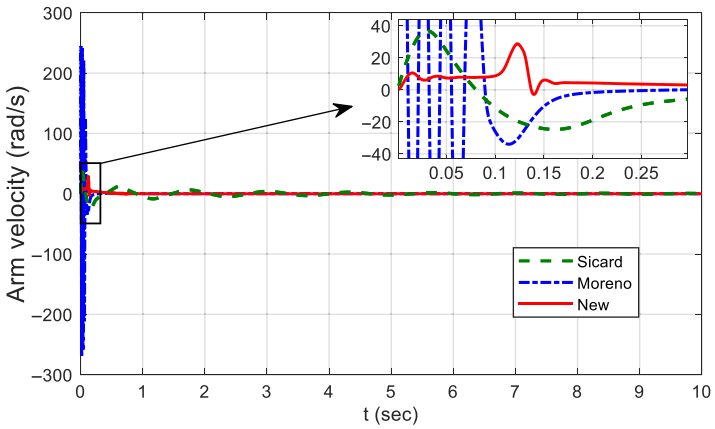


Fig. 5. The angular velocity of the arm in comparison with three implemented controllers.

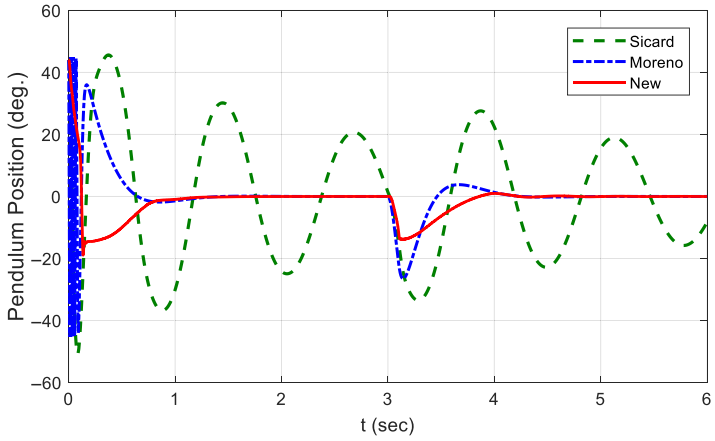


Fig. 6. Pendulum position with external disturbance.

To check the robustness of the controller, an external disturbance as a torque is applied to the pendulum for 0.1 s with $F_d = 0.5$ *NM* and the controller behavior is evaluated. Pendulum position has been shown in Fig. 6 and quantification of the error with disturbance has been evaluated in Table V.

According to Fig. 6, external disturbance can significantly deviate the pendulum angle relative to its vertical position. The designed robust controller compensates for the disturbance effect and keeps the pendulum in the vertical position. The overshoot of the response after disturbance is lower than the previous methods and settling time highlights the controller adaptability. The RMS values of the errors in Table V show the ability of the proposed controller in disturbance rejection in comparison with other approaches.

4.3.1. Various initial pendulum positions analysis. In the following, the different initial position of the pendulum has been investigated. As has been referred before, the fuzzy technique has been used to able the controller to stabilize the pendulum for bigger deviations from zero. According to Section 4.3, the biggest initial angle in which other approaches work is 44° but in Fig. 7, it is demonstrated that the proposed approach can stabilize the pendulum from 60° as well. To show the performance of the controller the pendulum position and the arm velocity for three initial positions of the pendulum

https://doi.org/10.1017/S0263574720001125 Published online by Cambridge University Press

Table VI. Quantification of results in various initial pendulum positions.

	30°	**45°**	**60°**
Settling time $q_1(t)$ (2%) [s]	0.787	1.0284	1.0432
RMS {U(t)}[Nm]	3.2226	9.7321	39.1052

Table VII. Quantification results of comparison of the proposed Dual ANN-Fuzzy controller, ANN controller, and Dual ANN controller.

	ANN	**Dual ANN**	**Dual ANN-Fuzzy (proposed)**
RMS error (deg.)	4.8115	5.0644	4.6285
RMS {U(t)}[Nm]	53.5929	4.3875	2.6313

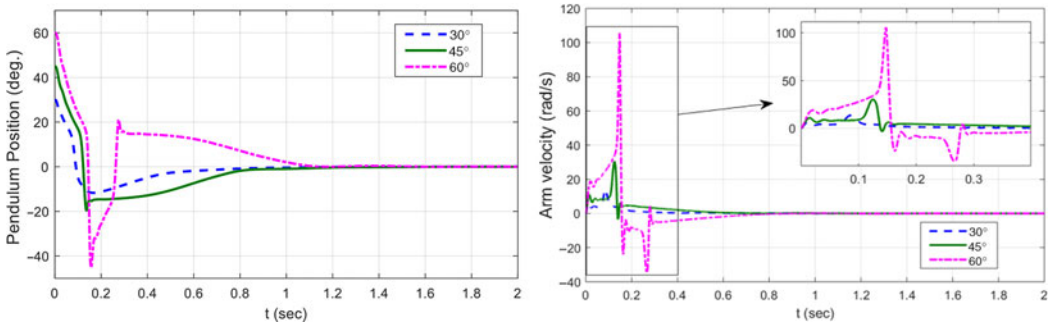


Fig. 7. Pendulum position and arm velocity in various initial pendulum positions.

are shown in Fig. 7. For quantitative comparison, the settling time and the RMS values of the control input are indicated in Table VI.

As seen in Fig. 7 and Table VI, three initial positions (30, 45, and 60°) of the pendulum have been analyzed. It is clearly shown that in smaller deviations from zero, the control input and settling time are smaller as well. The leveraging fuzzy technique not only enables the controller to stabilize the robot from a big initial deviation of zero, but also the position error, settling time, and the control input has a reasonable amount.

4.3.2. Corrective control analysis. In the following section, applying the fuzzy technique in (33) and adding U_{cor} which is the second part of the controller in (18) has been investigated. One of the advantages of the presented approach is using a dual neural network to eliminate oscillations, which are emerged by a discontinuity of the sign function which is used in other approaches like.[19,46] The fuzzy technique is used to remove the limit of the initial position of the pendulum, but as it is shown in Fig. 8 and Table VII, it modified the error and control input as well. To show the effect of the U_{cor} in oscillation compensation, the results with U_{cor} and without that has been shown in Fig. 8 and Table VII. Actually, the Dual ANN controller, which is proposed in (18) that is just without fuzzy technique in (33) and the ANN controller, which is compared with them is defined by

$$U_2 = \hat{W}^T \sigma\left(\hat{V}^T x\right) + K_v r + sign(r), \tag{57}$$

where the Dual ANN-Fuzzy is the presented approach in this paper. Figure 8 and Table VII show the performance of the proposed algorithm in comparison with the ANN controller without U_{cor} and the proposed controller without the fuzzy technique. The proposed control scheme has compensated the oscillation caused by uncertainties and discontinuity. Although by multiplying a coefficient to the sign function, the pendulum position oscillation could be decreased (not eliminated at all), but the control input value increases, so that it becomes unreasonable. The results suggest that the performance of the proposed algorithm is clearly better than the performance of the ANN controller which is formulated in (57).

https://doi.org/10.1017/S0263574720001125 Published online by Cambridge University Press

Table VIII. Quantification of results.

	AFSMC	**Dual ANN**
RMS $\{\mathbf{e_1}(t)\}$ (deg.)	56.6244	20.0680
Max $\{\lvert\mathbf{e_1}(t)\rvert\}$ (deg.) , 1.5<t<3	0.0945	0.0381
RMS {U(*t*)}(Nm)	1.2956	1.3153
Settling time $\boldsymbol{q_1}(t)$ (2%) (s)	0.704	0.225

Table IX. Quantification results of comparison of the proposed Dual ANN controller and AFSMC controller.

	AFSMC	**Dual ANN**
RMS error (deg.)	49.1839	18.0820
RMS {U(t)}(Nm)	8.0465	1.9307

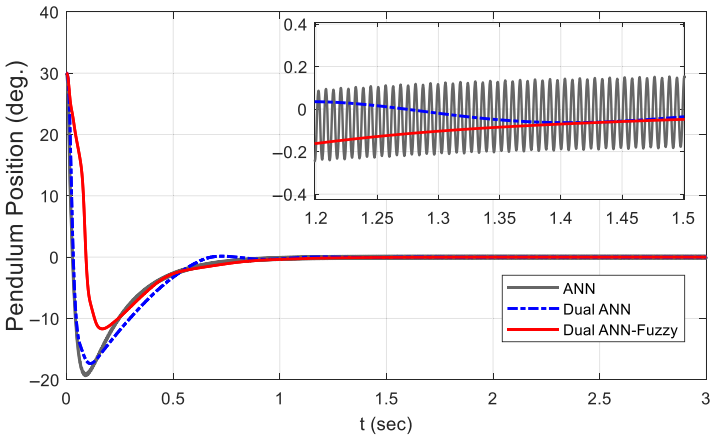


Fig. 8. The angle of pendulum position. Proposed Dual ANN-Fuzzy controller in comparison with ANN controller and Dual ANN controller.

The controller is able to drive the Furuta pendulum system toward its desired equilibrium points (i.e., *X=0*) in an efficient manner. Simulation results clearly show the stabilizing ability of the controller. Thus, the algorithm can be used for either of two-degrees-of-freedom systems with a slight design modification.

4.4. Simulation results for the Inertia wheel pendulum

In this section, the effectiveness of the proposed Dual ANN method is assessed in controlling the underactuated dynamic model of the Inertia Wheel Pendulum (IWP) system. In the first part of this section, disturbances are not taken into account but in the second part, the performance of the controller is being tested in the presence of a step disturbance input. The proposed controller in (34) is labeled as "Dual ANN" and the controller introduced by[39] in (52) as a free model controller is labeled as "AFSMC". The results of reaching the inverted pendulum to the vertical position from 175° without external disturbances were shown in Fig. 9. The maximum absolute value of the pendulum position error, the Root Mean Square (RMS) value of the error, and the control input and the settling time were compared in Table VIII. In maximum error quantification, the chosen time interval was 1.5s, when the pendulum is in a stable position, and the maximum of the error has been highlighted.

To examine the effect of disturbances on the performance of this system, a step function has been exerted in the second time of the simulation for 0.1s with $F_d = 7\ NM$. The desired values were the same as before. In Figs. 10 and 11, the performance of the system in the presence of disturbance is depicted for the pendulum angle and wheel velocity, respectively. Quantification of the error with disturbance has been presented in Table IX.

As it is shown in Fig. 10, the same disturbance caused different deviations because of different controllers. For the AFSMC controller, the pendulum angle after applying the disturbance reached to

https://doi.org/10.1017/S0263574720001125 Published online by Cambridge University Press

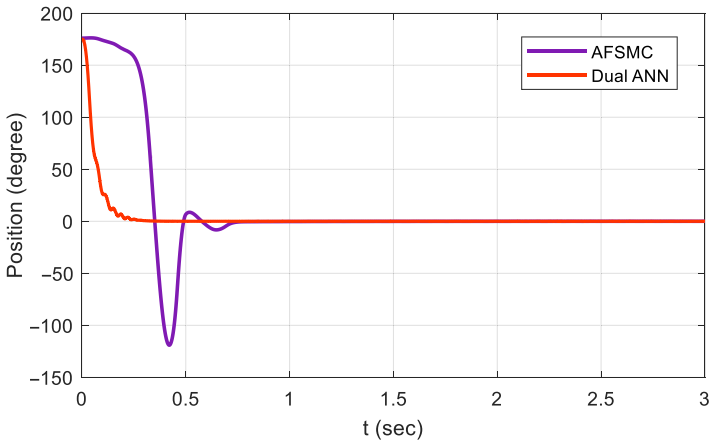


Fig. 9. The angle of pendulum position in comparison with another implemented controller.

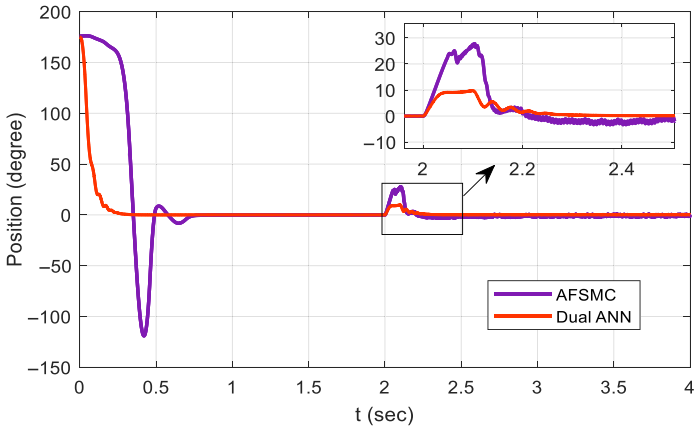


Fig. 10. Pendulum position with external disturbance.

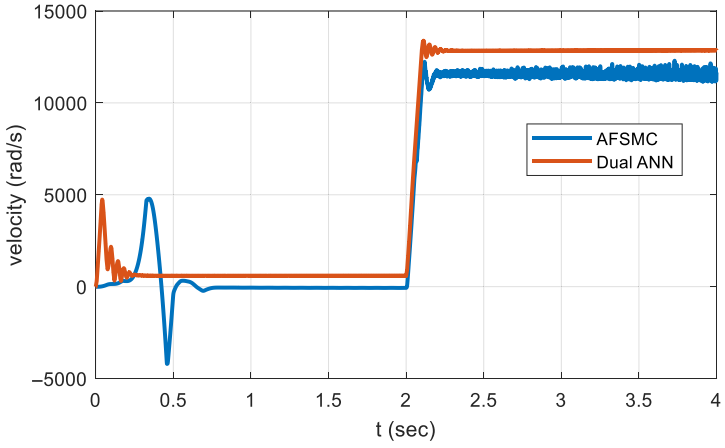


Fig. 11. Wheel velocity with external disturbance.

28° while this number for Dual ANN was 9.8°. The figures show that there is no significant chattering after the pendulum reached to the neighborhood of the desired values. However, Fig. 11 depicts that the system experiences a high wheel velocity after the exertion of the disturbance. The results showed that the proposed controller has a good performance in various underactuated systems and it is robust under plant uncertainties and exogenous disturbances.

https://doi.org/10.1017/S0263574720001125 Published online by Cambridge University Press

5. Conclusion

This paper has discussed nonlinear robust control based on dual adaptive neural network for underactuated systems. Two underactuated systems including robot Furuta and Inertia Wheel Pendulum (IWP) have been considered for implementing the proposed approach to achieve both swings up and balancing. The Dual-ANN strategy reduces the dependency of the control approach to the plant model and it is robust under plant uncertainties and exogenous disturbances. Such advantages are obtained by using a fuzzy technique, which is continuously tuned by observing the deviations of the pendulum from the desired value, and also by continuously estimating the bound of uncertainties by an adaptive approach. The U_{cor} was introduced to compensate for the oscillation of the pendulum when it reaches the desired point. The controller was derived from the universal approximation property of neural networks, and weight adaptation laws were designed. The simulation results distinctly show the performance of the proposed control law in uncertain nonlinear underactuated systems. The results have been compared with previous works to highlight the efficiency of the proposed approach. Besides, the presented algorithm can be easily extended for any other two degrees of freedom underactuated system. The authors are planning to investigate different ordering of the adaptive neural network and other activation functions to increase the efficiency and to apply the proposed approach in other complex systems for future works.

Acknowledgements

We would also like to show our gratitude to the reviewers and Chief editor of the journal for their comments on an earlier version of the manuscript.

Conflict of Interest

The authors declare that they have no conflict of interest.

References

1. F. Pourboghrat and M. Karlsson, "Adaptive control of dynamic mobile robots with nonholonomic constraints," *Comput. Electr. Eng*. **28**(4), 241–253 (2002).
2. S. Labiod and M. S. Boucherit, "Adaptive fuzzy control of a class of MIMO nonlinear systems," *Fuzzy Sets. Syst*. **151**(1), 59–77 (2005).
3. K. W. Lee and K. Hassan, "Adaptive output feedback control of robot manipulators using high-gain observer," *Int. J. Control*. **67**(6), 869–886 (1997).
4. R. A. DeCarlo, S. H. Zak and G. P. Matthews, "Variable structure control of nonlinear multivariable systems: A tutorial," *Proc. IEEE*. **76**(3), 212–232 (1988).
5. Y. Stepanenko, Y. Cao and C.-Y. Su, "Variable structure control of robotic manipulator with PID sliding surfaces," *Int. J. Robust Nonlinear Control* **8**(1), 79–90 (1998).
6. A. L. Elshafei and F. Karray, "Variable-structure-based fuzzy-logic identification of a class of nonlinear systems," *IEEE Trans. Control Syst. Technol*. **13**(4), 646–653 (2005).
7. C. Kwan and F. L. Lewis, "Robust backstepping control of nonlinear systems using neural networks," *IEEE Trans. Syst. Man. Cybern Part A Syst. Hum*. **30**(6), 753–766 (2000).
8. G. W. Lee and F. T. Cheng, "Robust control of manipulators using the computed torque plus H8 compensation method," *IEE Proc. Control Theory Appl*. **143**(1), 64–72 (1996).
9. S. Zabihifar and A. Yushchenko, "Управление двухзвенным манипулятором с использованием нечеткого управления скользящего типа," *Вестник Московского государственного технического университета им. НЭ Баумана. Серия «Приборостроение»* **105**(6), 30–45 (2015).
10. S. Zabihifar and A. Yushchenko, "Hybrid force/position control of a collaborative parallel robot using adaptive neural network," *International Conference on Interactive Collaborative Robotics* (Leipzig, Germany, 2018) pp. 280–290.
11. J. Nelson and L. G. Kraft, "Real-time control of an inverted pendulum system using complementary neural network and optimal techniques," *American Control Conference*, (Baltimore, 1994) pp. 2553–2554.
12. S. Cong and Y. Liang, "PID-like neural network nonlinear adaptive control for uncertain multivariable motion control systems," *IEEE Trans. Ind. Electron*. **56**(10), 3872–3879 (2009).
13. C.-F. Hsu, "Adaptive backstepping Elman-based neural control for unknown nonlinear systems," *Neurocomputing* **136**, 170–179 (2014).
14. C.-F. Hsu, C.-M. Lin and R.-G. Yeh, "Supervisory adaptive dynamic RBF-based neural-fuzzy control system design for unknown nonlinear systems," *Appl. Soft. Comput*. **13**, 1620–1626 (2013).
15. Z. Ping, "Tracking problems of a spherical inverted pendulum via neural network enhanced design," *Neurocomputing* **106**, 137–147 (2013).
16. M. W. Spong, P. Corke and R. Lozano, "Nonlinear control of the reaction wheel pendulum," *Automatica* **37**(11), 1845–1851 (2001).

https://doi.org/10.1017/S0263574720001125 Published online by Cambridge University Press

17. S. Kurode and C. Asif, "Swing-up and stabilization of rotary inverted pendulum using sliding modes," *IFAC Proc.* **44**(1), 10685–10690 (2011).
18. R. Shubhobrata and B. Ranjit Kumar, "Stabilization of furuta pendulum: A backstepping based hierarchical sliding mode approach with disturbance estimation," *7th International Conference on Intelligent Systems and Control (ISCO)* (Coimbatore, India, 2013) pp. 99–105.
19. J. Moreno-Valenzuela, "Adaptive Neural Network Control for the Trajectory Tracking of the Furuta Pendulum," *IEEE Trans Cybern.*, 3439–3452 (2016).
20. K. Furuta, M. Yamakita and S. Kobayashi, "Swing-up Control of Inverted Pendulum," *International Conference on Industrial Electronics, Control and Instrumentation* (Kobe, Japan, 1991) pp. 2193–2198.
21. Y.-F. Huang and A.-C. Chen, "Adaptive control of rotary inverted pendulum system with time-varying uncertainties," *Springer* **76**(1), 1112–1114 (2013).
22. J. Acosta, "Furuta's pendulum: A conservative nonlinear model for theory and practice," *Math. Probl. Eng*. **2010**, 1–29 (2010).
23. C. Aguilar-Ibañez, M. Suárez-Castañon and O. Gutiérres-Frias, "The direct Lyapunov method for the stabilization of the Furuta pendulum," *Int. J. Control* **83**(11) 2285–2293 (2010).
24. T. Turker, H. Gorgun and G. Cansever, "Lyapunov's direct method for stabilization of the Furuta pendulum," *Turk J. Electr. Eng. Comput. Sci*. **120**(1) 99–110 (2012).
25. J. de Jesús Rubio, "Discrete time control based in neural networks for pendulums," *Appl. Soft. Comput. J*. **68**, 821–832 (2018).
26. K. Astrom, J. Aracil and F. Gordillo, "A family of smooth controller for swinging up a pendulum," *Automatica* **36**(2), 1841–1848 (2008).
27. F. Gordillo, J. Acosta and J. Aracil, "A new swing-up law for the Furuta pendulum," *Int. J. Control* **76**(8), 836–844 (2003).
28. P. Hera, L. Freidovich, A. Shiriaev and U. Mettin, "New approach for swing up the Furuta pendulum: Theory and experiments," *Mechatronics* **19**, 1240–1250 (2009).
29. R. Hercus and K.-y. Wong, "Control of an Inverted Pendulum using the NeuraBase," *International Conference on Neural Information Processing* (Springer, Berlin, Heidelberg, 2013) pp. 605–615.
30. L. Aguilar, I. Boiko, L. Fridman and R. Iriarte, "Generating self-excited oscillations via two-relay controller," *IEEE Trans. Autom. Control* **54**(2), 416–420 (2009).
31. L. Freidovich, A. Shiriaev, F. Gordillo, F. Gomez-Estern and J. Aracil, "Partial-energy-shaping control for orbital stabilization of high-frequency oscillations of the Furuta pendulum," *IEEE Trans. Control Syst. Technol*. **17**(4), 853–858 (2009).
32. P. Sicard and H. Chaoui, "Motion and Balance Neural Control of Inverted Pendulums with Nonlinear Friction and Disturbance," *Proceedings of the 24th Canadian Conference on Electrical and Computer Engineering, CCECE 2011, Niagara Falls* (Canada, May 2011) pp. 001222–001227.
33. C. Yu, F. Wang and Y. Lu, "Robust control of a Furuta pendulum," *SICE Annual Conference* (Taipei, Taiwan, 2010) pp. 2559–2563.
34. M. Khanesar, M. Teshnehlab and M. Shoorehdeli, "Fuzzy sliding mode control of rotary inverted pendulum," *IEEE International Conference on Computational Cybernetics* (Gammarth, Tunisia, 2007) pp. 57–62.
35. P. Van Cuong and W. Yao Nan, "Adaptive trajectory tracking neural network control with robust compensator for robot manipulators," *Nat. Comput. Appl*. **27**, 525–536 (2016).
36. H. Boudjedir, F. Yacef, O. Bouhalim and A. Rizoug, "Dual neural network for adaptive sliding mode control of quadrotor helicopter stabilization," *IJIST* **2**, 1–14 (2012).
37. F. W. Lewis, S. Jagannathan and A. Yesildirak, *Neural Network Control Of Robot Manipulators And Non-Linear Systems* (CRC press, Boca Raton, FL, 1998).
38. S. Shuzhi, S. Ge, C. C. Hang, T. H. Lee and T. Zhang, *Stable Adaptive Neural Network Control* (Springer US, Berlin, Germany, 2002).
39. S. Zabihifar, A. H. Davaie Markazi, M. Madani and N. Doostmohammadi, "Adaptive fuzzy sliding mode control of under-actuated nonlinear systems," *Int. J. Autom. Comput*. **15**, 364–376 (2018).
40. I. Fantoni, *Non-linear Control for Underactuated Mechanical Systems* (Springer, London, 2002).
41. R. Olfati-Saber, "Fixed point controllers and stabilization of the cart-pole system and the rotating pendulum," *Proc. 38th IEEE Conf. Decis. Control* **2**, 1174–1181 (1999).
42. V. Santibañez, R. Kelly and J. Sandoval, "Control of the Inertia Wheel Pendulum by Bounded Torques," *Proceedings of the 44th IEEE Conference on Decision and Control* (Seville, Spain, 2005) pp. 8266–8270.
43. S. Kim and S. S. Jung, "Control experiment of a wheel-driven mobile inverted pendulum using neural network," *IEEE Trans. Control Syst. Technol*. **16**(2), 297–303 (2008).
44. S. George and L. Feng, "Adaptive neural network control by adaptive interaction," *Proceedings of the American Control Conference* (Arlington, VA, 2001) pp. 1247–1252.
45. D. B. Robert and L. Feng, "Adaptive interaction and its application to neural networks," *Inf. Sci*. **121**(3), 201–215 (1999).
46. S. Kurode and C. Asif, "Swing-Up and Stabilization of Rotary Inverted Pendulum using Sliding Modes," *International Federation of Accountan* (Milano, 2011) pp. 10685–10690.

https://doi.org/10.1017/S0263574720001125 Published online by Cambridge University Press